Optics and other considerations for coherent x-ray beamlines

Ian McNulty

Center for Nanoscale Materials, ANL

Argonne National Laboratory

19 November 2014

Coherence

Temporal (longitudinal) coherence

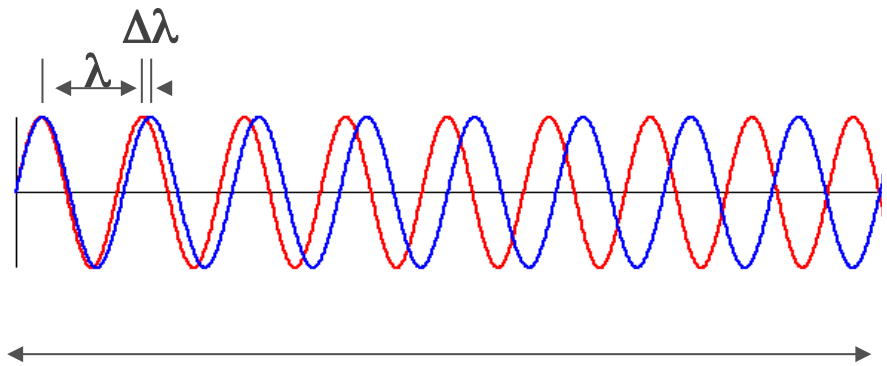

$$l_c \sim \frac{\lambda^2}{\Delta\lambda}$$

$$\tau_c \sim \frac{\lambda^2}{c\Delta\lambda}$$

Spatial (transverse) coherence

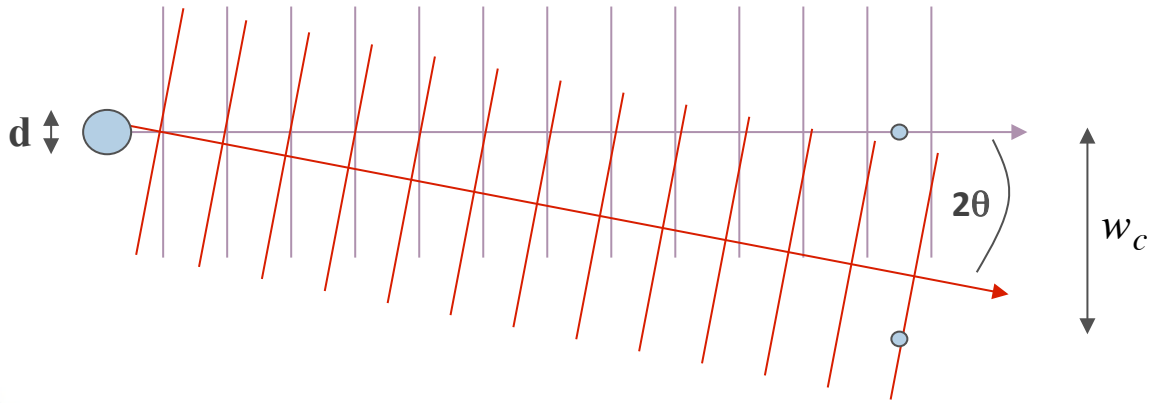

$$w_c \sim \frac{\lambda z}{d}$$

$$d \cdot \theta = \lambda / 2\pi$$

$$\Delta x \, \Delta p \geq \hbar / 2$$

Synchrotron radiation

- SR sources (except FEL) are incoherent, but highly forward directed due to relativistic effects $\theta \sim 1/\gamma$

- Spatial and temporal filtering (pinholes, monochromators) are needed to select the coherent flux $F_c \sim \lambda^2 B$

- Only the coherent flux can be focused into a diffraction-limited spot or be used to form interference fringes

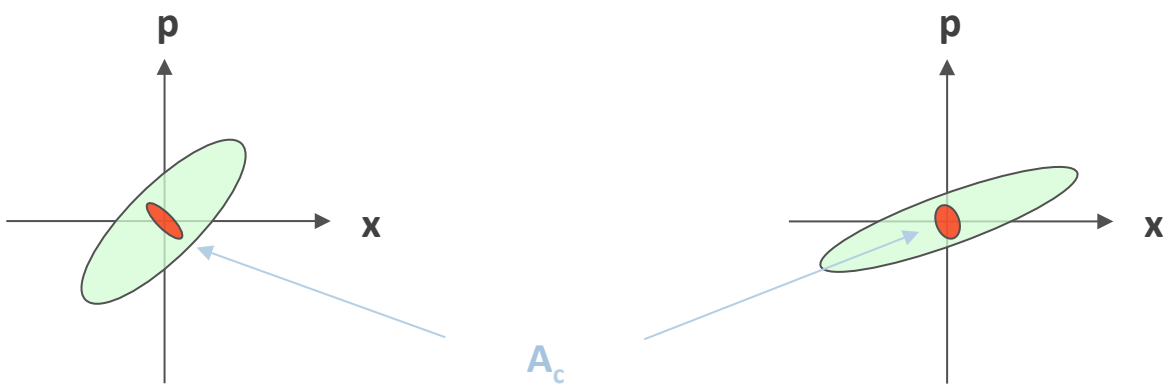

Coherent vs. total flux of SR sources

Flux per spatially coherent mode: $F_c = B\,\lambda^2/4$

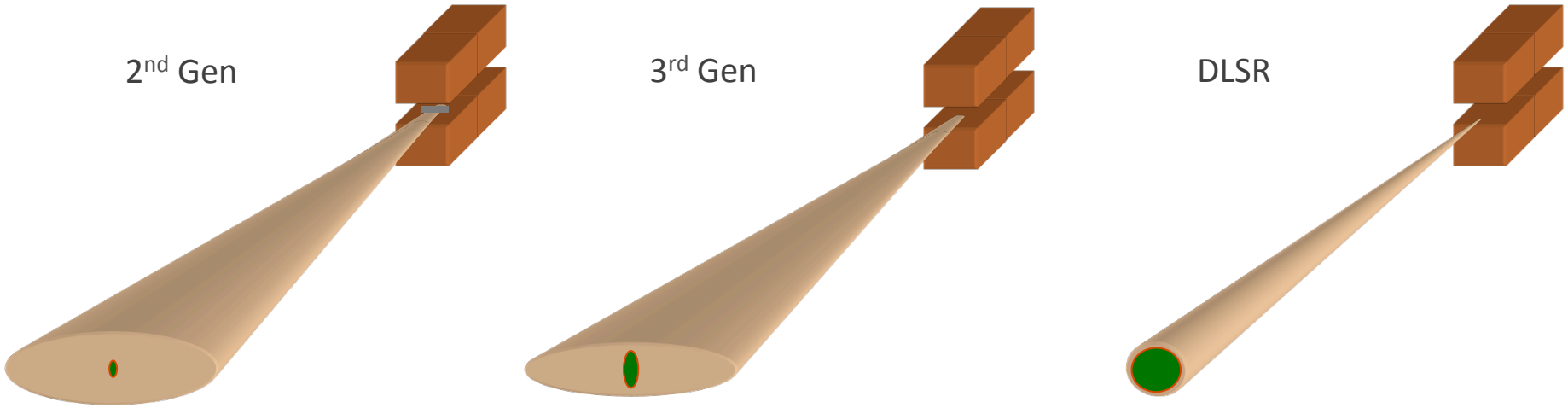

Large emittance, low brilliance,
small coherent fraction and flux

Small emittance, high brilliance,
large coherent fraction and flux

APS brightness with MBA lattice

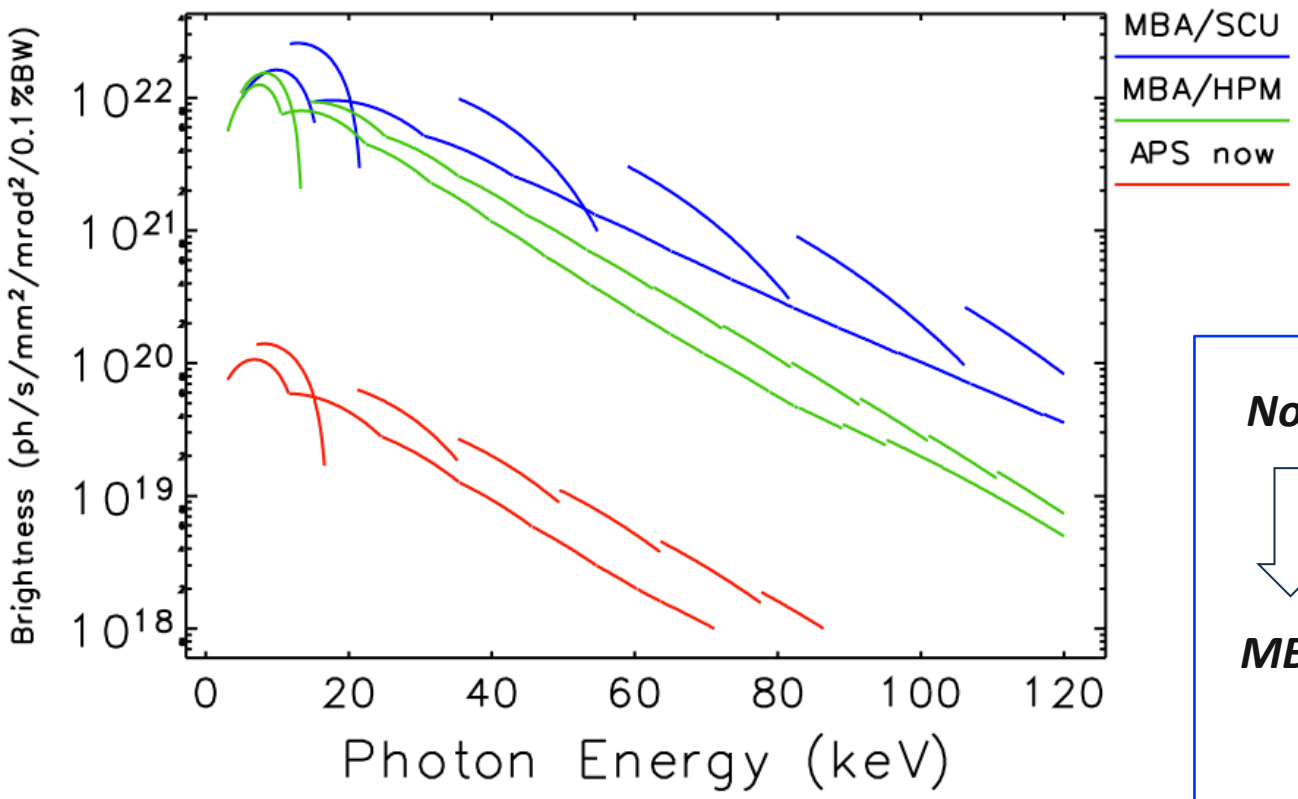

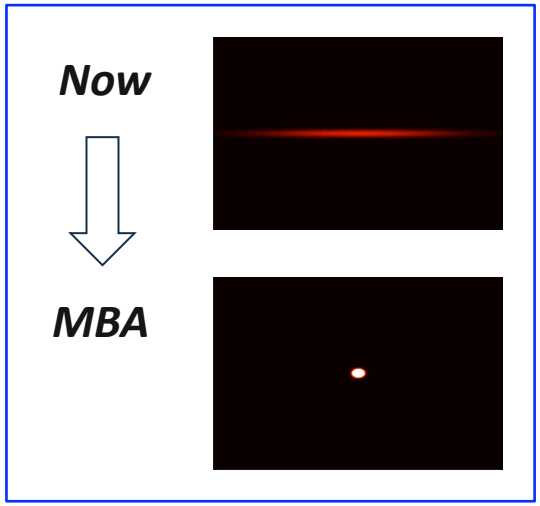

Figure 1: Comparison of brightness from the present APS to selected hybrid-permanent magnet and superconducting undulators in the MBA lattice design described here.

M. Borland (ANL)

Imaging resolution by x-ray holography

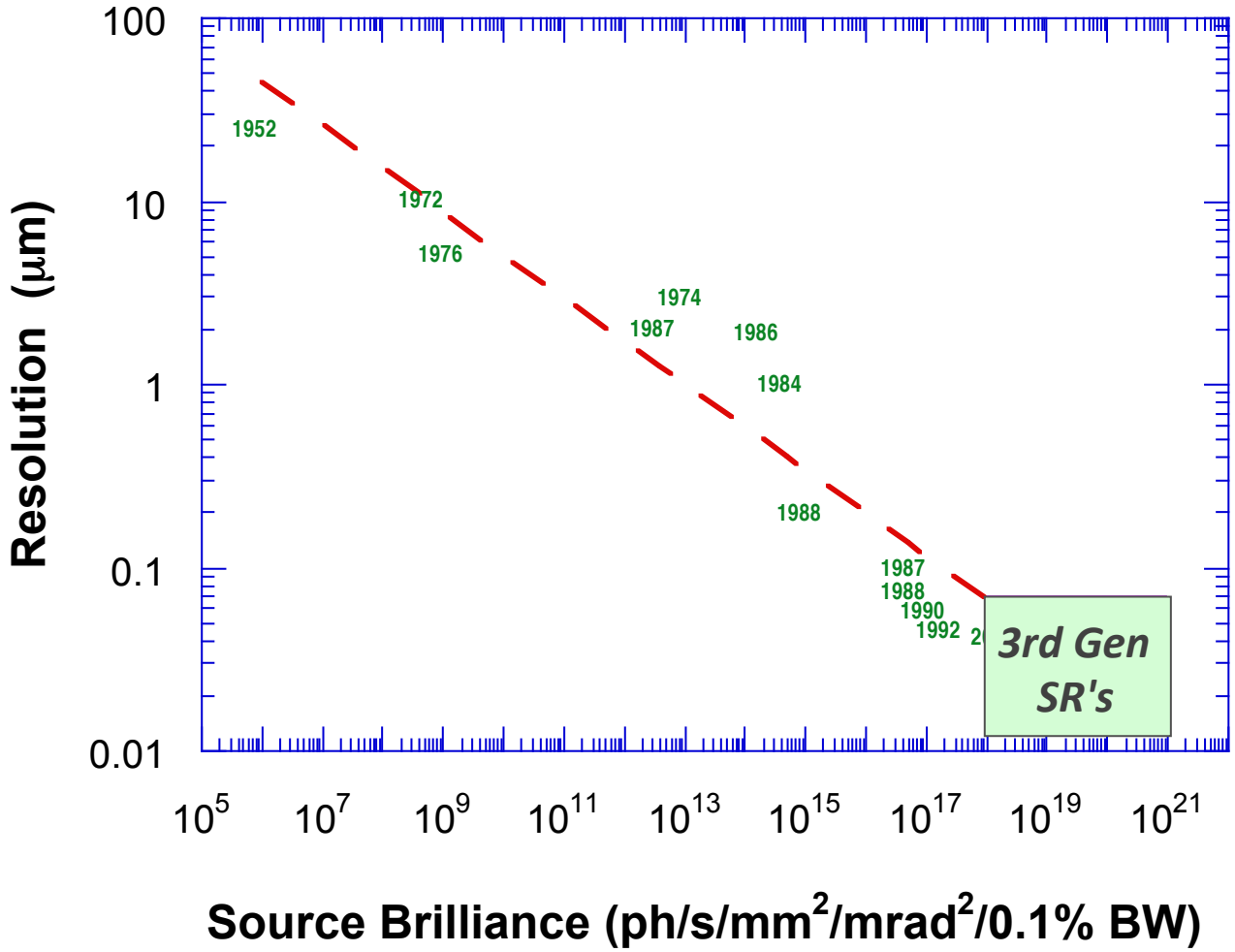

X-ray scattering from a disordered sample

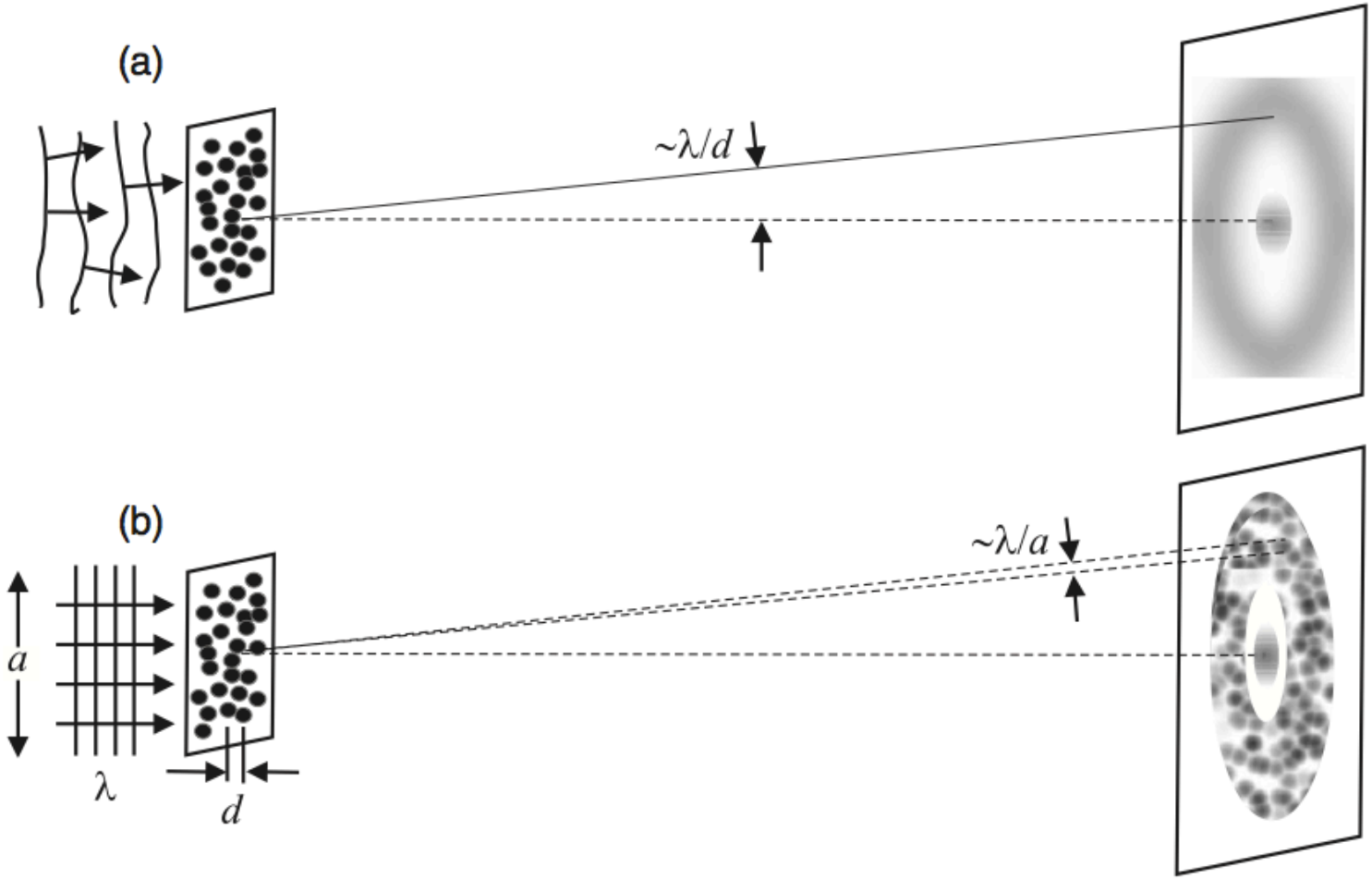

X-ray diffraction from a disordered medium with particle distance d and object size a
(a) **Incoherent scattering**, giving rise to a continuous diffraction ring
(b) **Coherent scattering**, resulting in a speckled diffraction ring

F. van der Veen, F. Pfeiffer, J. Phys. Cond. Mater. 16, 5003 (2004)

Coherent vs. incoherent

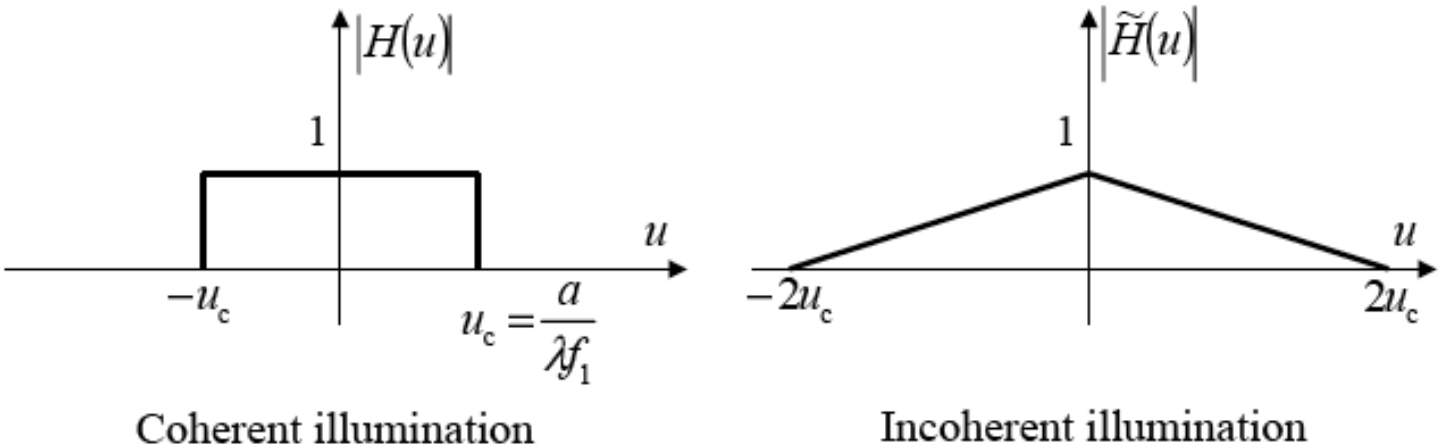

Scanning and full-field microscopy are *incoherent* methods

- Transfer function is linear in the field *intensities*
- Characterized by sloping function down to 2NA

Diffraction and holographic microscopy are *coherent* methods

- Transfer function is linear in the field *amplitudes*
- Characterized by flat top, sharp cutoff at limiting NA

Coherence "degradation" from bad optics?

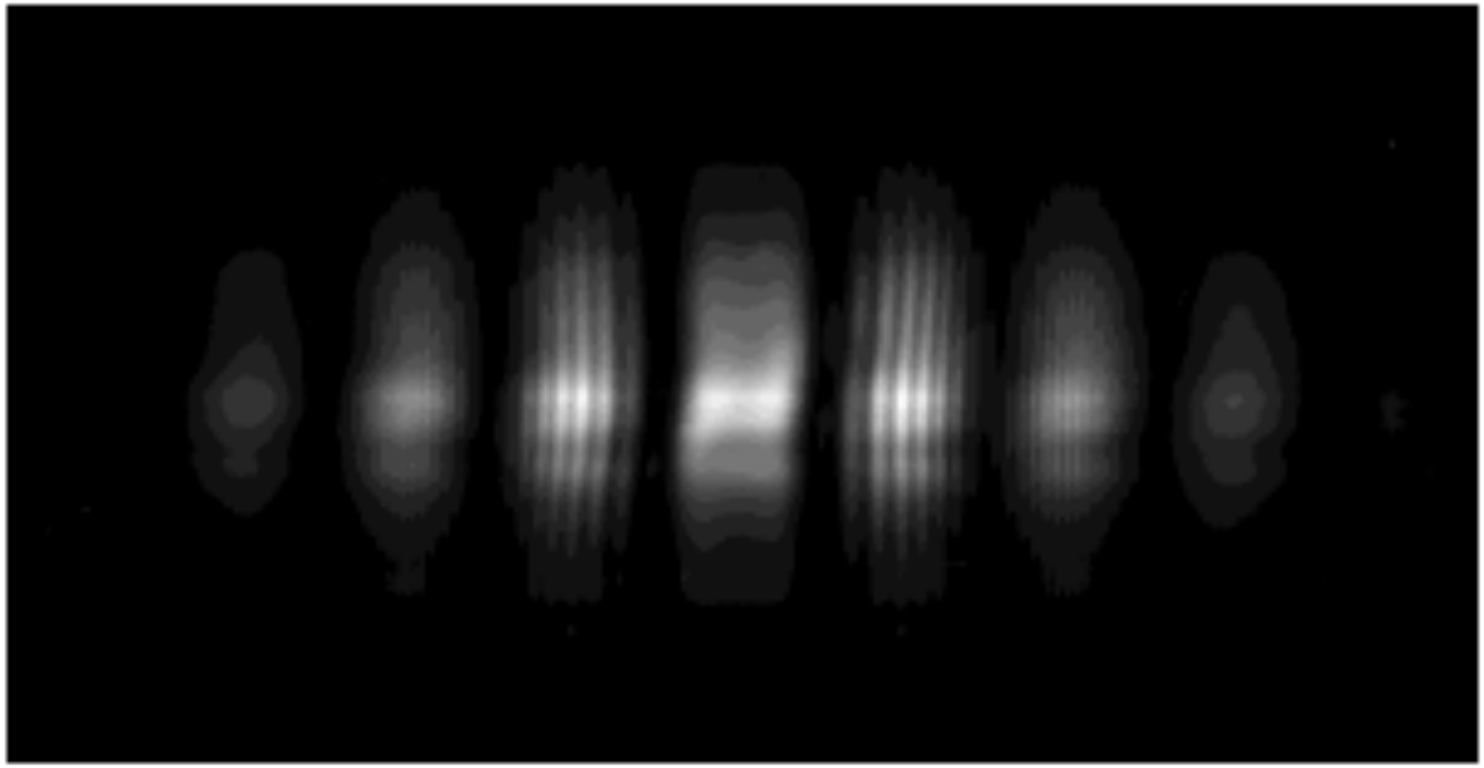

CCD image of Young's interference pattern with 10 µm slit separation at 1.07 m, using 1.5 keV x-rays. Image is 820 µm by 420 µm and fringe spacing is 90 µm.

Condition for full utilization of coherence by experiment: $d_{aperture} < d_{speckle}$

Preserving coherence

- First Law: "Do no harm"
  - Minimum use of apertures: every edge makes fringes
  - Best quality optics: maintain wavefront quality
  - Stable optics!

- Second Law: "Provide tunable coherence properties"
  - Enable trade-off between coherence for flux
  - Adjustable coherence-selecting slits, ideally focusing too

- Third Law: "Use every drop!"
  - Coherence experiments are coherent-flux hungry
  - Experiments needing temporal as well as spatial coherence even more so (E^{-3} scaling)

Clean up beam with spatial filter

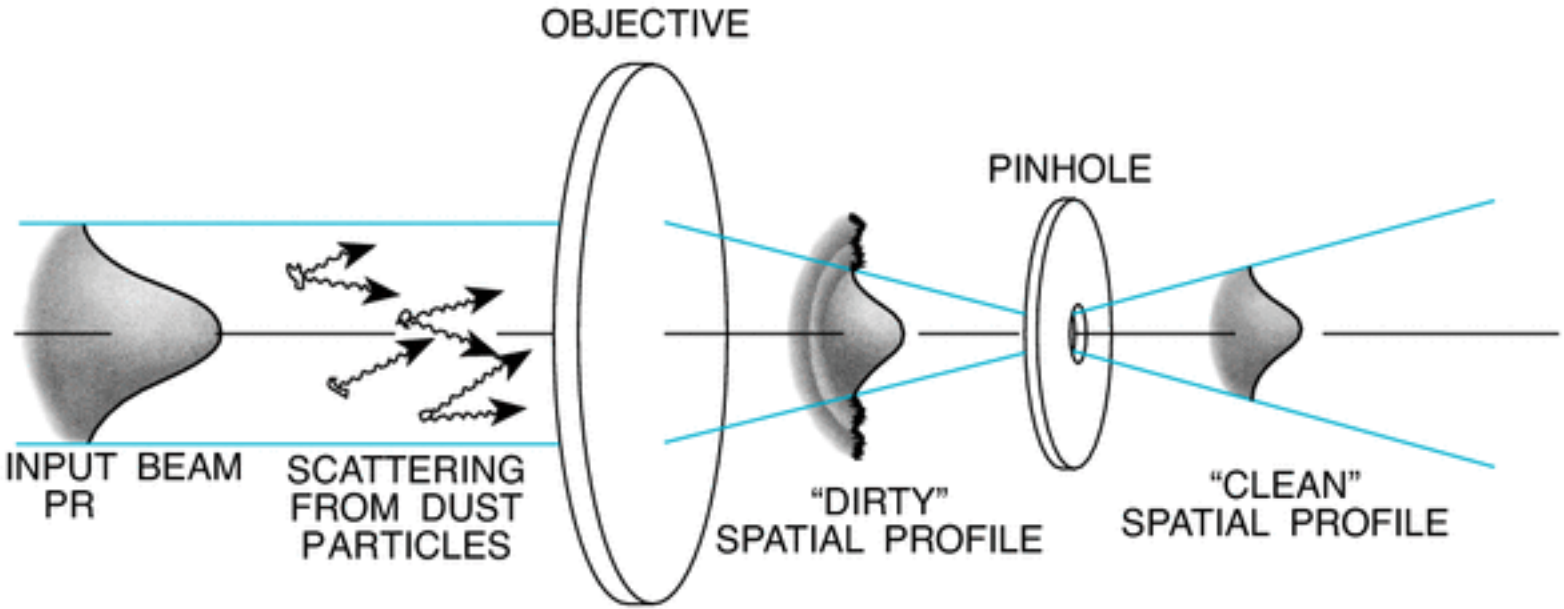

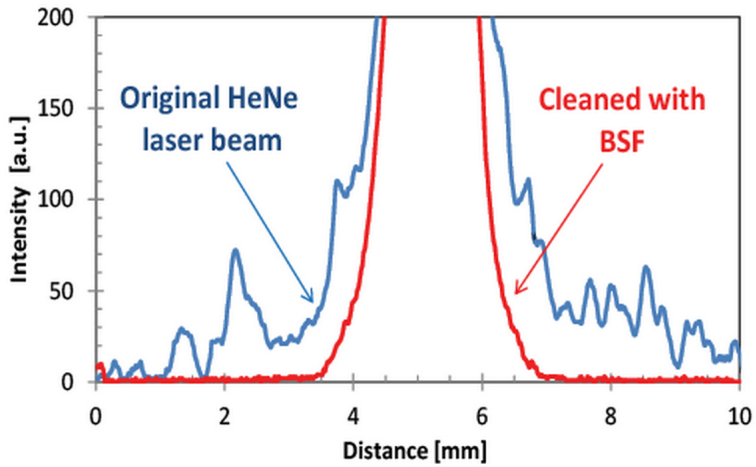

X-ray spatial filtering

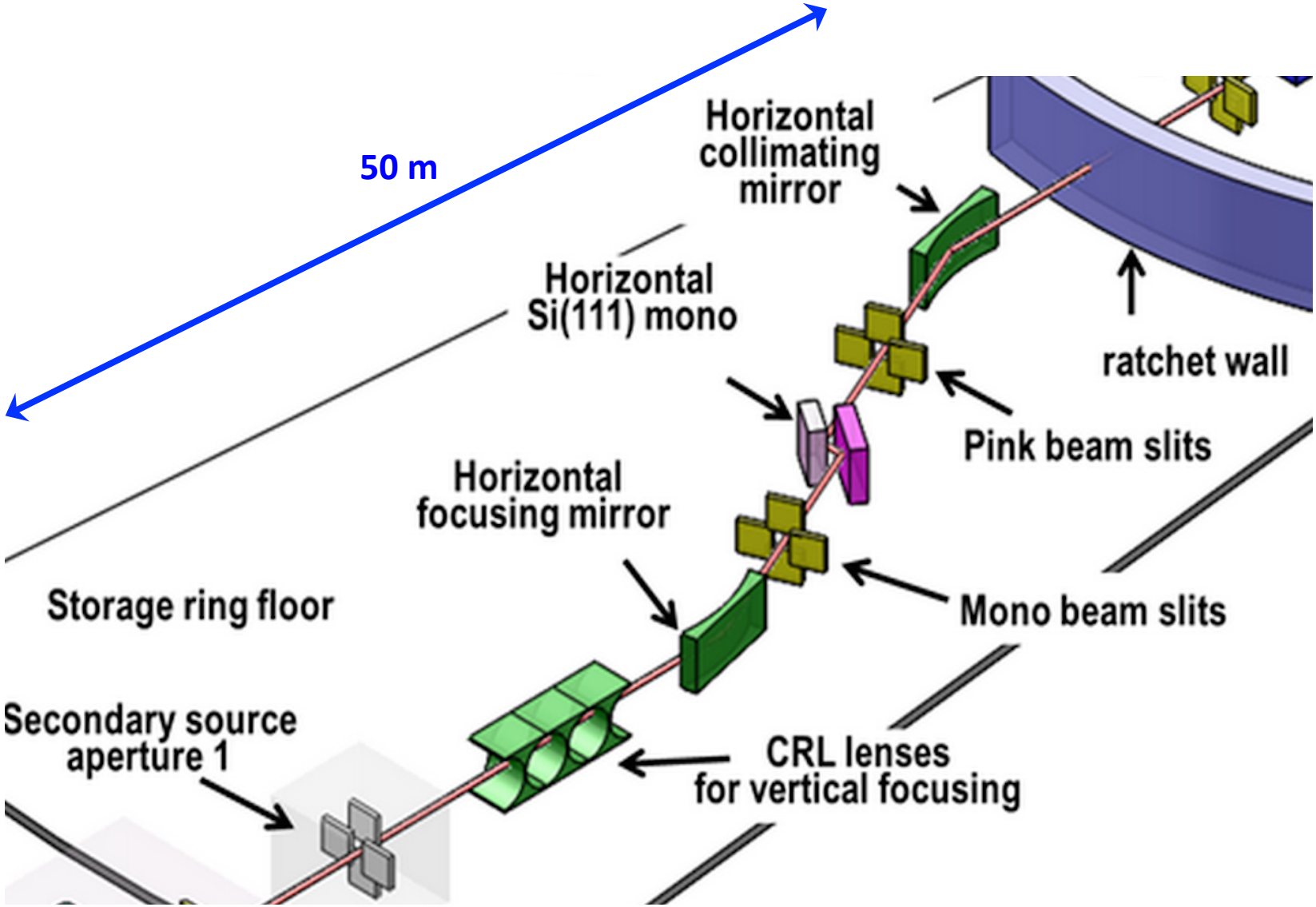

Beamlines for coherent x-rays: four classes

- 1st: Simple coherence selection (slit near source)
- 2nd: 1D spatial filtering (focusing onto slit)
- 3rd: 2D spatial filtering (stigmatic source, round beam)
- *4th: Modal control (optimize use of partial coherence)*

Coherence beamlines: 1st class

	Energy Range (keV)	Length (m)
▪ Soft x-ray		
– NSLS X1A (orig.)	0.2-0.8	26
– ALS 12.02	0.3-1.5	30
– BESSY UE-52	0.25-0.90	20
▪ Hard x-ray		
– ESRF ID10	7-30	69
– SPring8 BL29XUL	4-38	98
– APS 2-ID-D	5-30	72
– 8-ID-E/I	6-12	70
– 34-ID-C	6-12	53
– Petra 3 P10	4-25	90
– NSLS-II CHX*	6-15	80

UE56-SGM beamline and ALICE chamber at BESSY

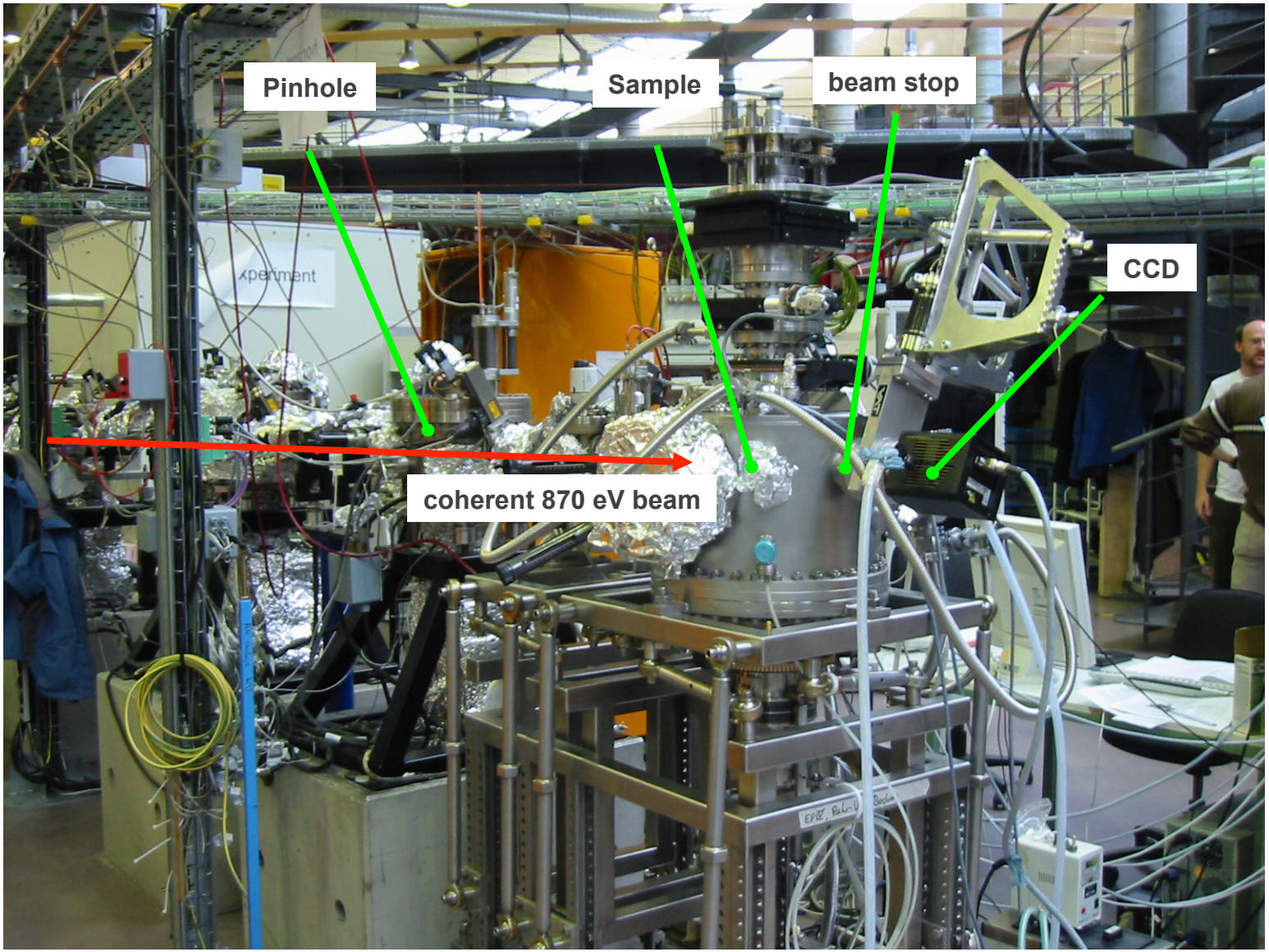

Coherence beamlines: 2nd class

	Energy Range (keV)	Length (m)
▪ "Conventional" length		
– APS 2-ID-B	1-4	62
– APS 26-ID	6-12	75
– Petra 3 P10	4-25	90
▪ "Long" beamlines		
– DLS I13	6-20	250

APS 2-ID-B beamline optics

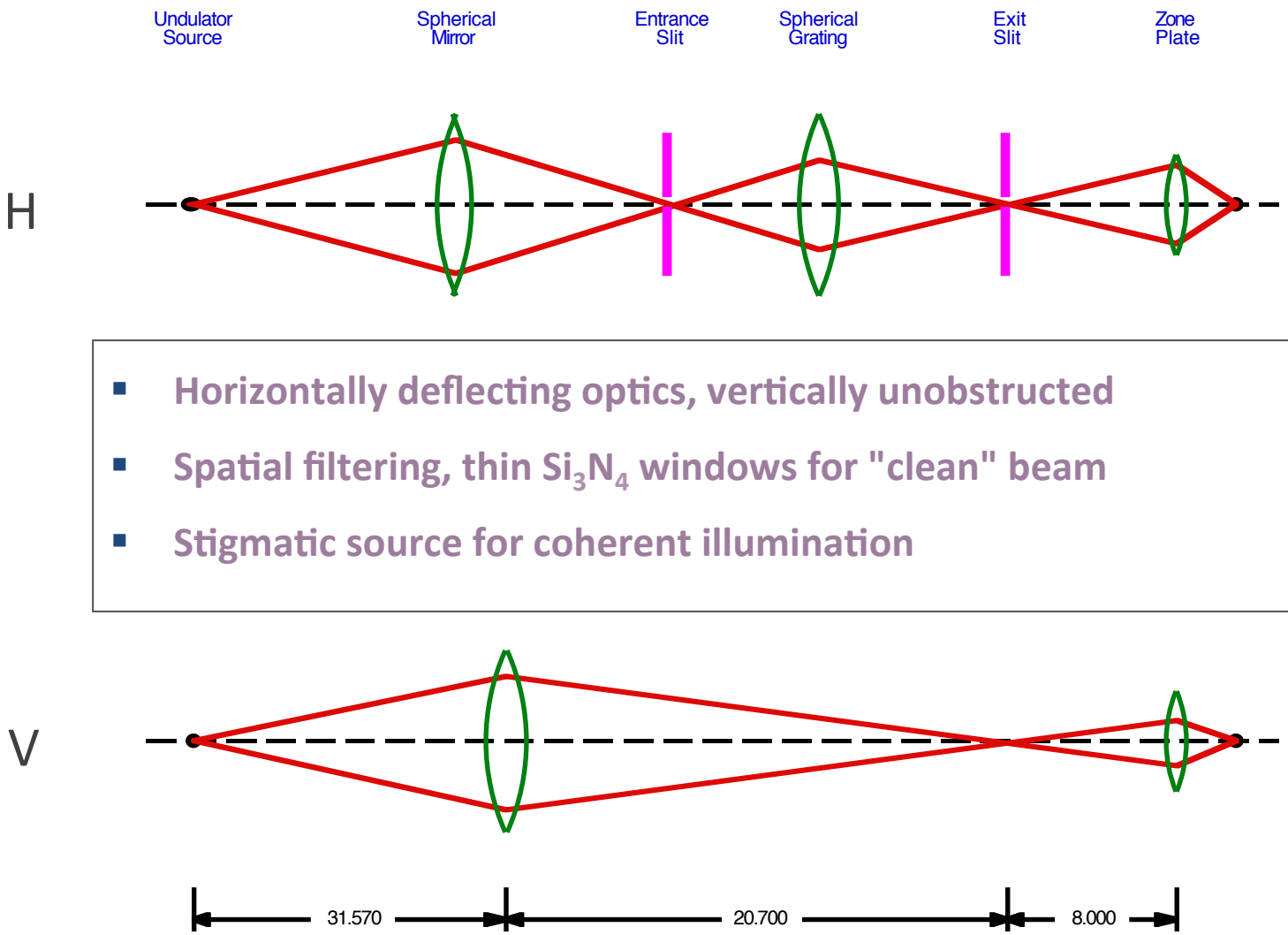

- Horizontally deflecting optics, vertically unobstructed
- Spatial filtering, thin Si_3N_4 windows for "clean" beam
- Stigmatic source for coherent illumination

I. McNulty, RSI 67, 3372 (1996)

Hard X-ray Nanoprobe at CNM/APS beamline 26-ID

Energy range: 6 – 12 keV
Focal spot: ~40 nm FWHM
Flux ~ 8×10^8 ph/s/0.1% BW
2-5 nm accuracy over 25 mm
< 2 nm/h positioning drift

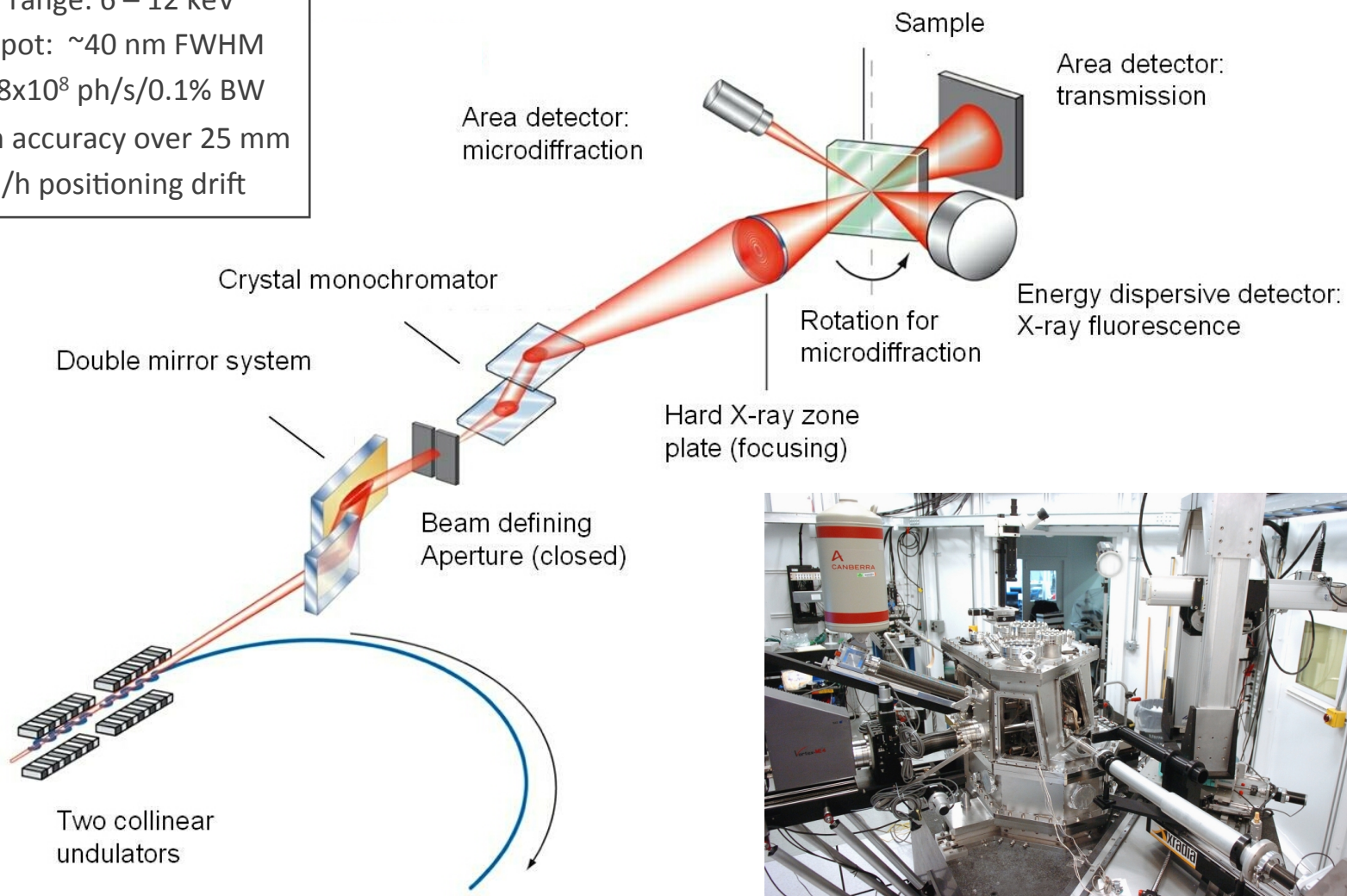

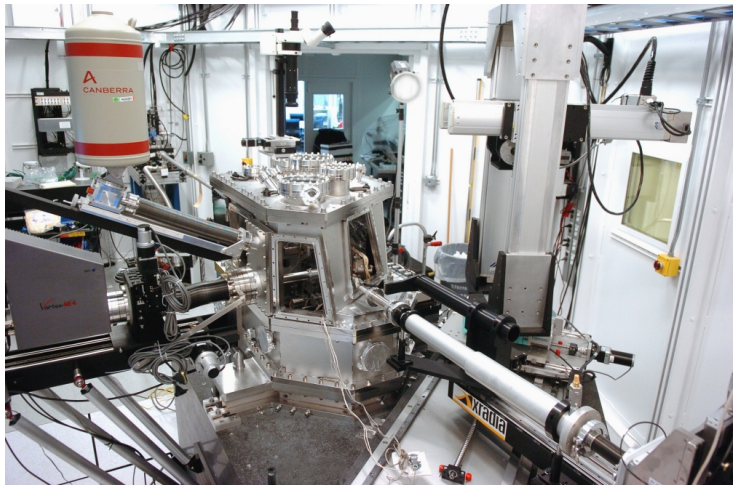

R.P. Winarski, JSR 19, 1056 (2012)

Coherence beamlines: 3rd class

	Energy Range (keV)	Length (m)
▪ "Conventional" length		
– Elettra Twin-Mic	0.4-2.2	27
– NSLS-II CSX	0.3-2	45
– SLS cSAXS	4-19	41
– Petra 3 P6	7-30	98
– ALS 7.0.1 (COSMIC) *	0.08-1.2	30
– TPS XNP*	4-15	69
– APS ISN*	4-30	70 -> 150 ?
▪ "Long" beamlines		
– Soleil Nanoscopium	5-20	155
– ESRF ID16A (NINA)	17-34	185
– MAX IV Nanomax*	5-30	95
– NSLS-II HXN*	6-25	108
– DLS I14*	4-30	~200

Elettra Twin-Mic beamline

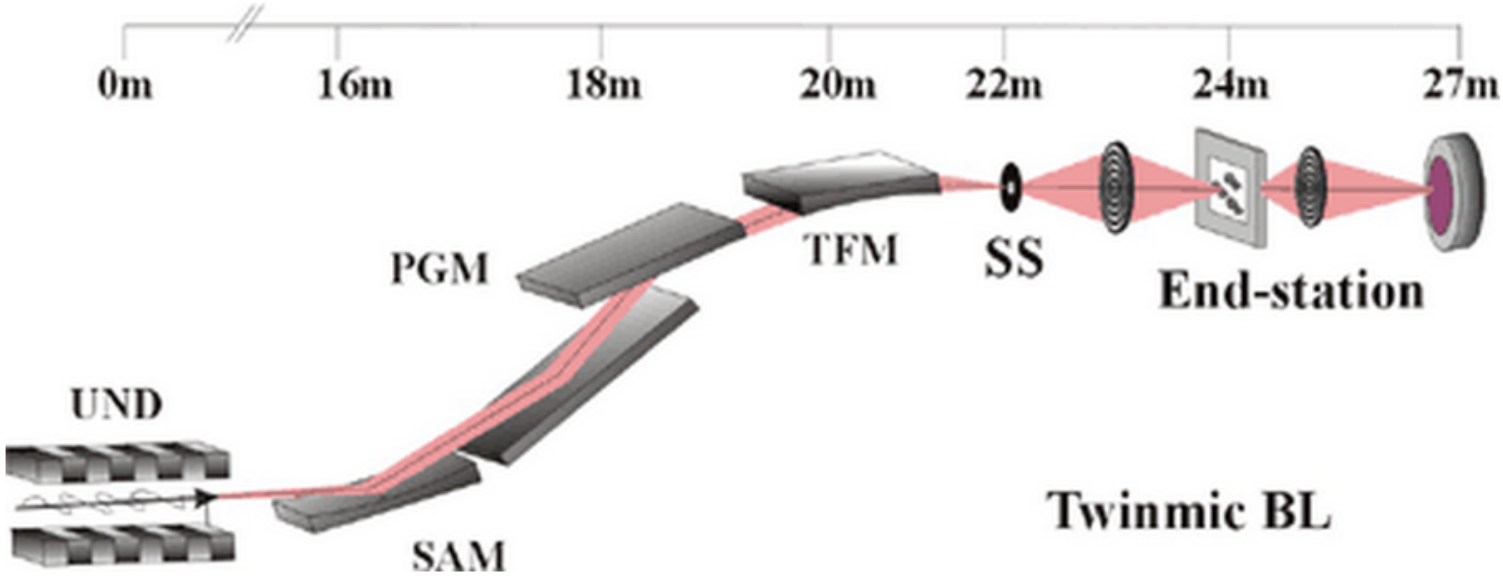

NSLS-II Coherent Soft X-ray beamline

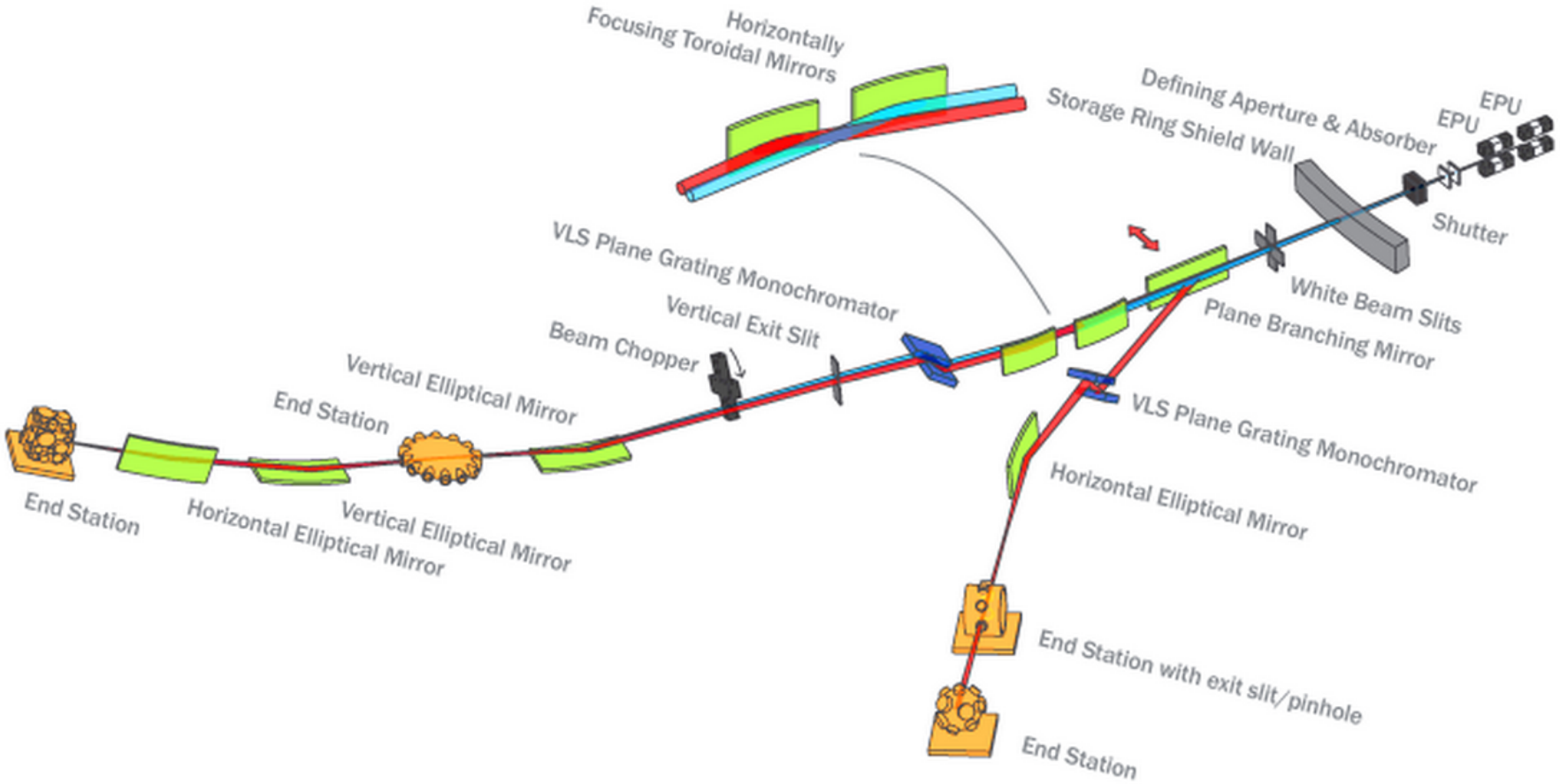

ALS COSMIC beamline

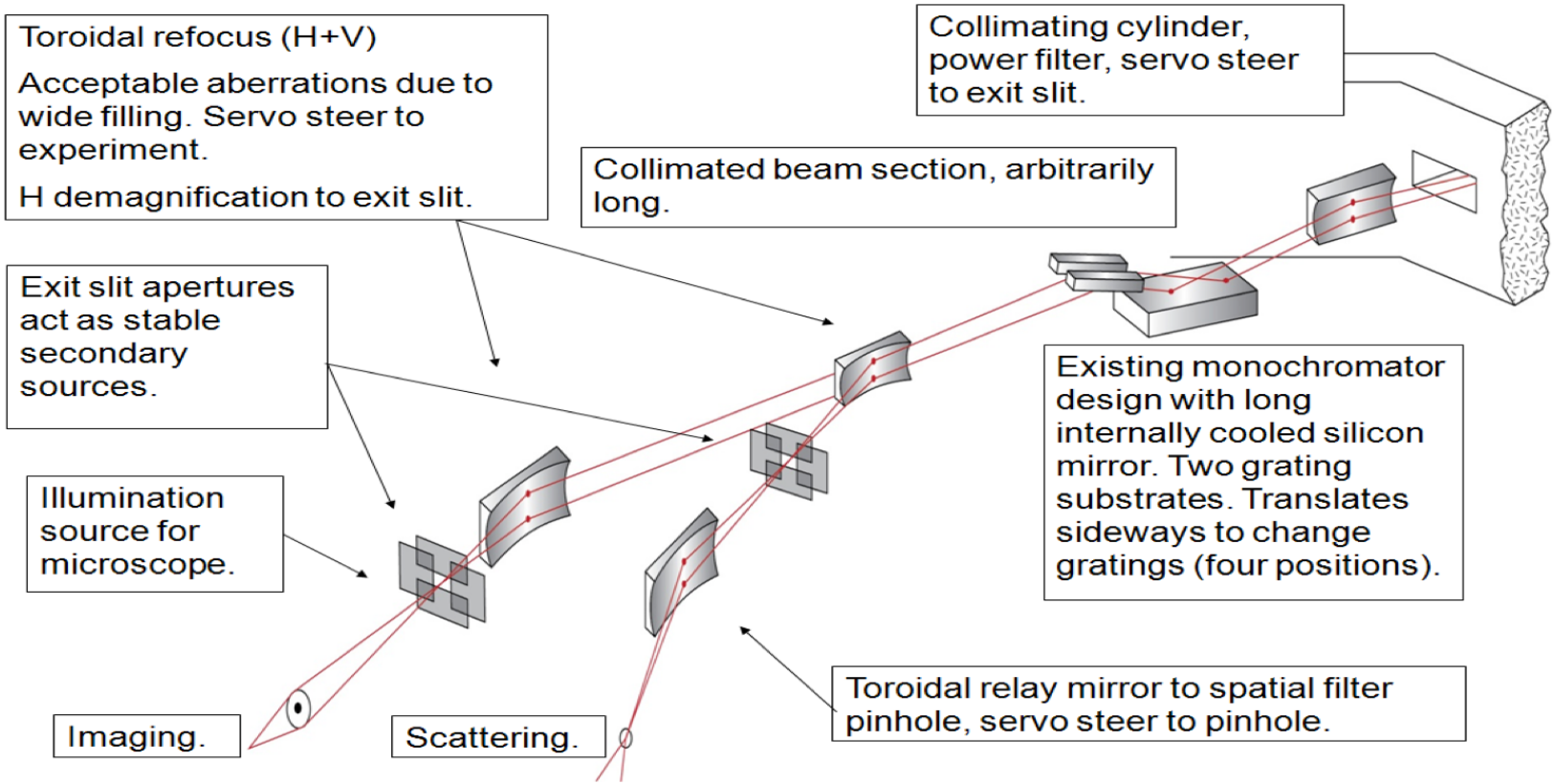

D. Shapiro, JPCS 425, 192011 (2013)

NSLS-II Hard X-ray Nanoprobe beamline

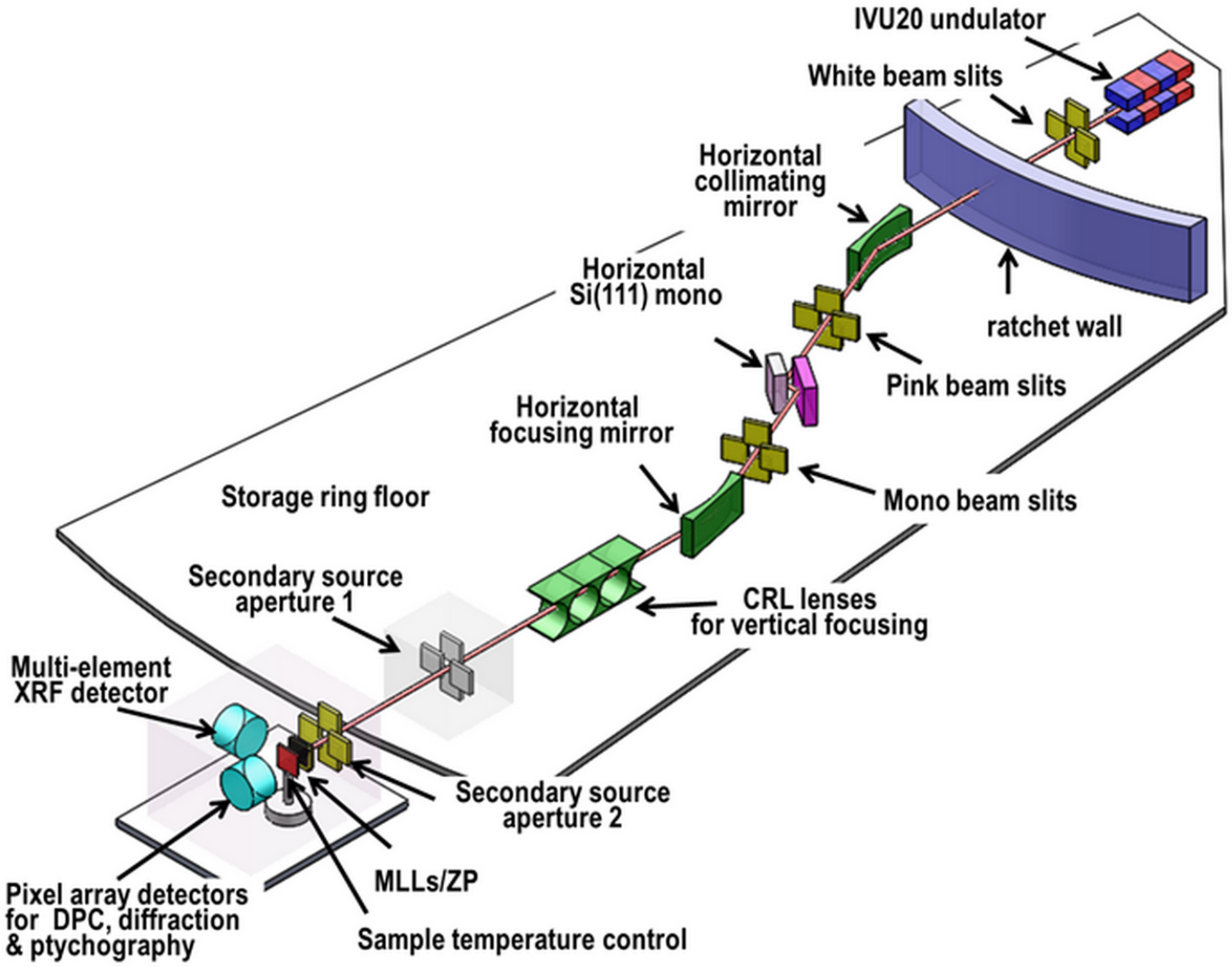

MAX IV Nanomax beamline

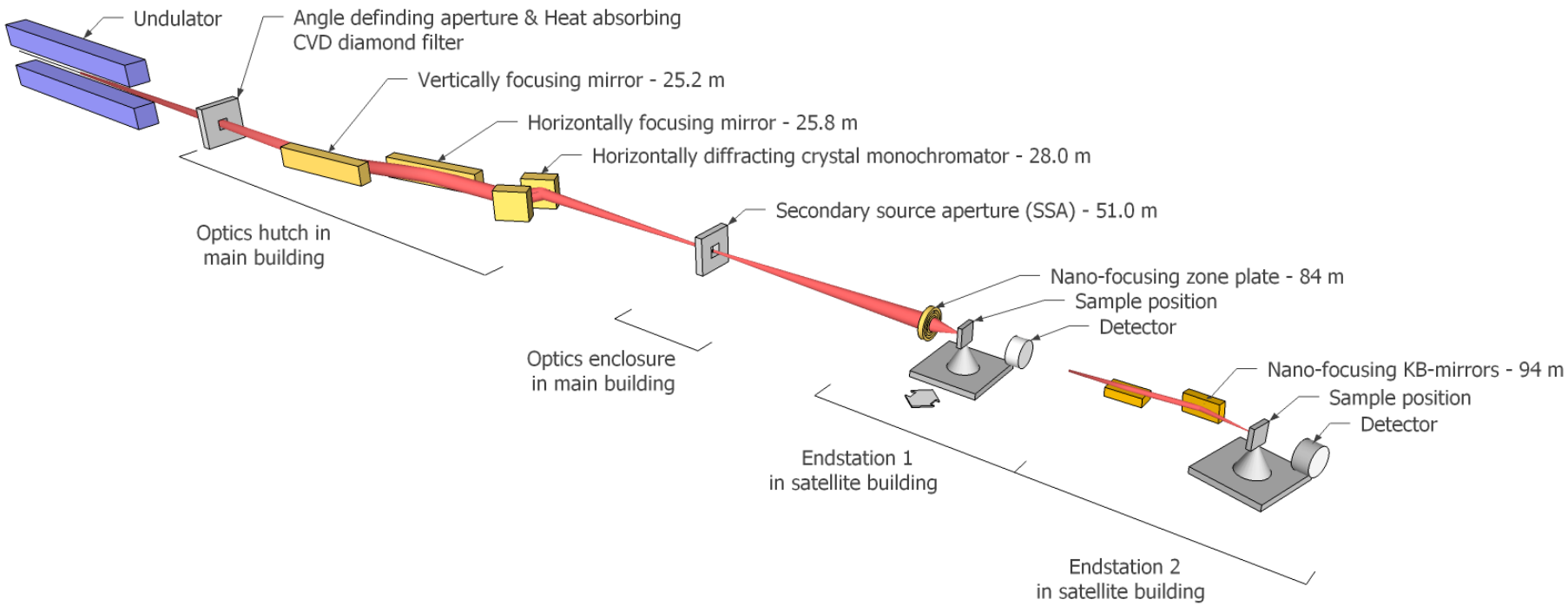

Coherent fraction of proposed DLSRs

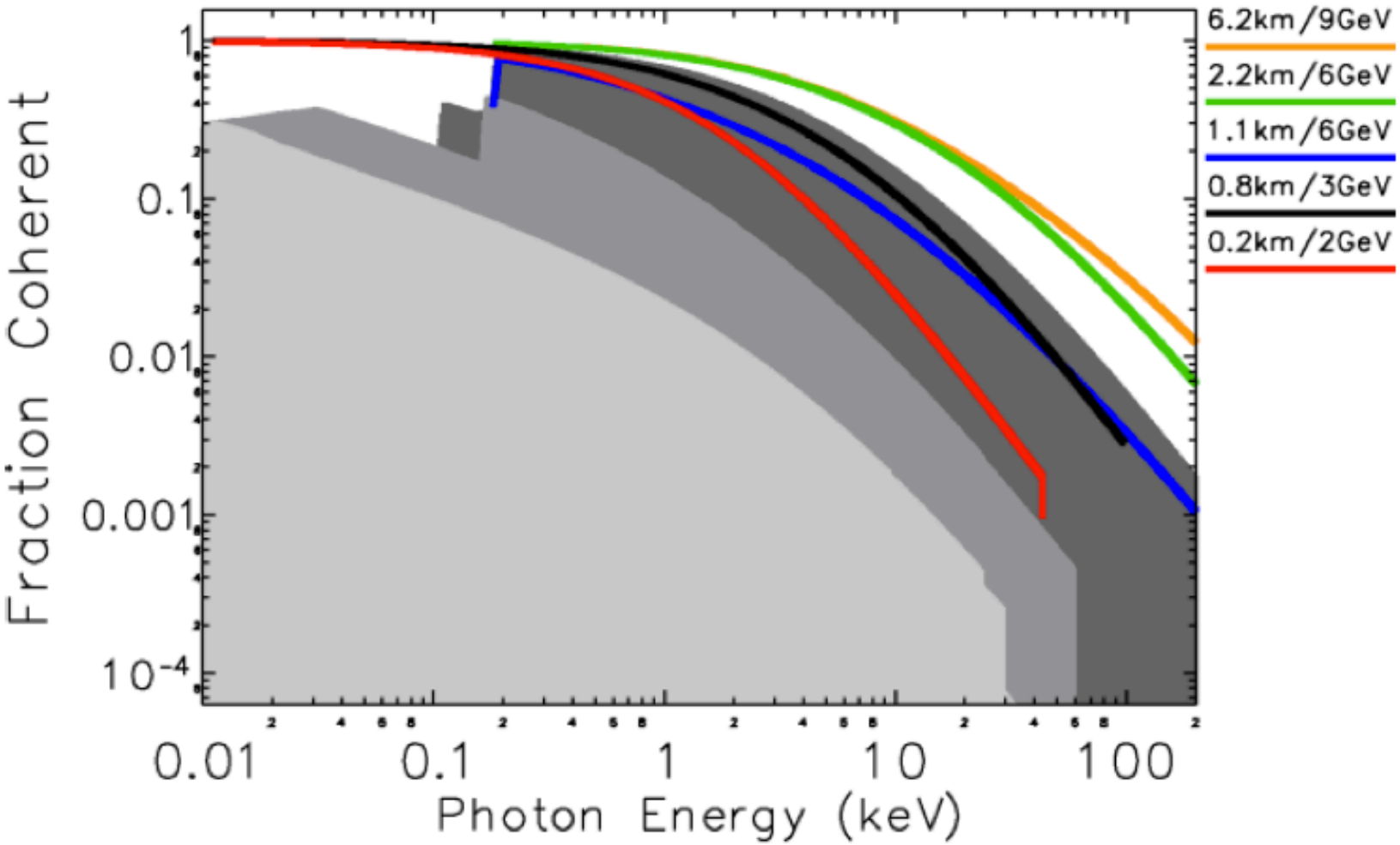

Partial coherent light can be treated as a distribution of coherent modes

$$J(\boldsymbol{r}_1, \boldsymbol{r}_2) = \sum_{n=1}^{N} \mu_n \psi_n(\boldsymbol{r}_1) \psi_n^*(\boldsymbol{r}_2),$$

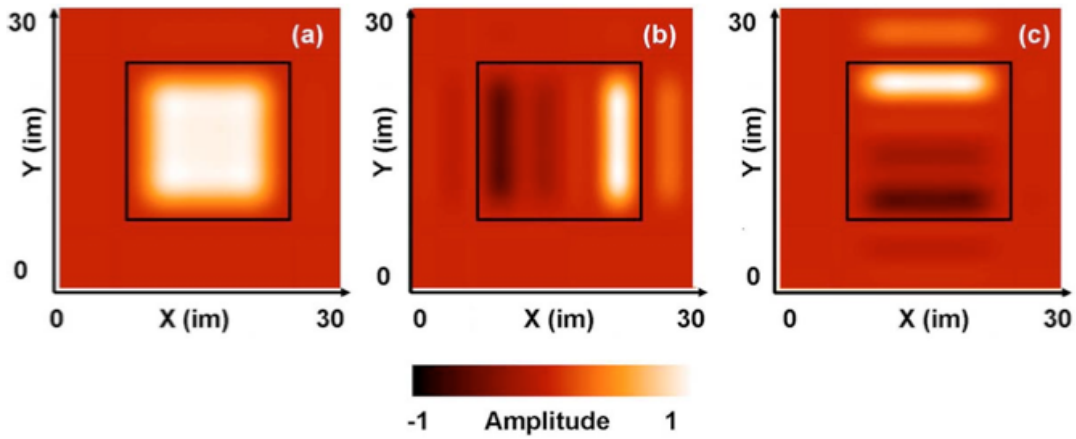

Coherent modes for the lower-coherence set of experimental data. The square delineates the edge of the physical aperture. (a) (0,0) mode, (b) (1,0) mode, (c) (0,1) mode.

S. Flewett, Opt. Lett 34, 2198 (2009)

Diffractive imaging with partially coherent light

- Conventional phase retrieval algorithms that assume full coherence break down with partially coherent light

$$I(\boldsymbol{k}) = \sum_{n=1}^{N} \mu_n I_n(\boldsymbol{k}),$$

- If you know (or guess) the modal distribution (i.e. its weighting μ_n), you can fold this into the algorithm to optimize for each mode

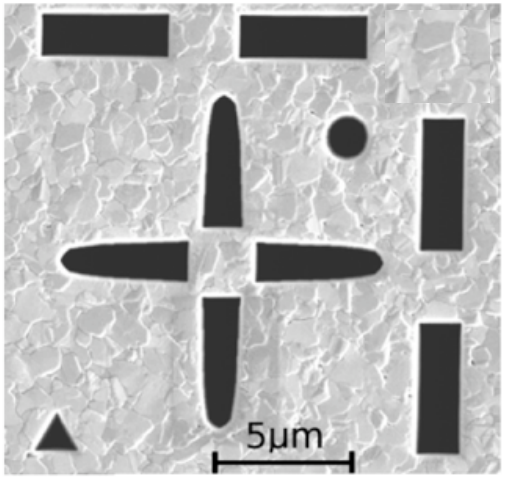

SEM of Au test pattern

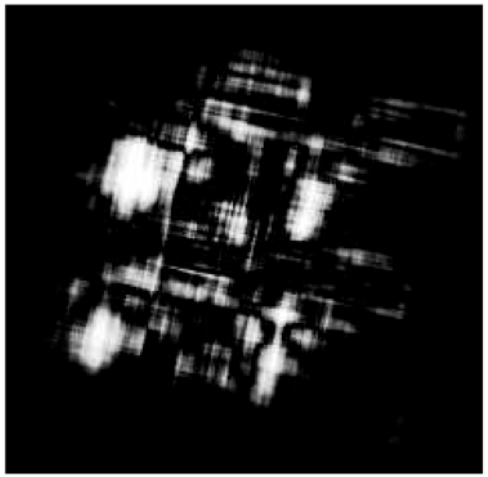

Conventional reconstruction with partial spatial coherence

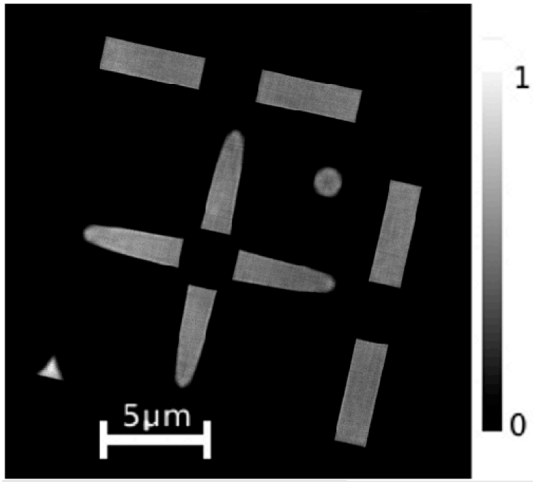

Reconstruction incorporating 3 spatially coherent modes

L. Whitehead, PRL 103, 243902 (2009)

Going broadband: use polychromatic light

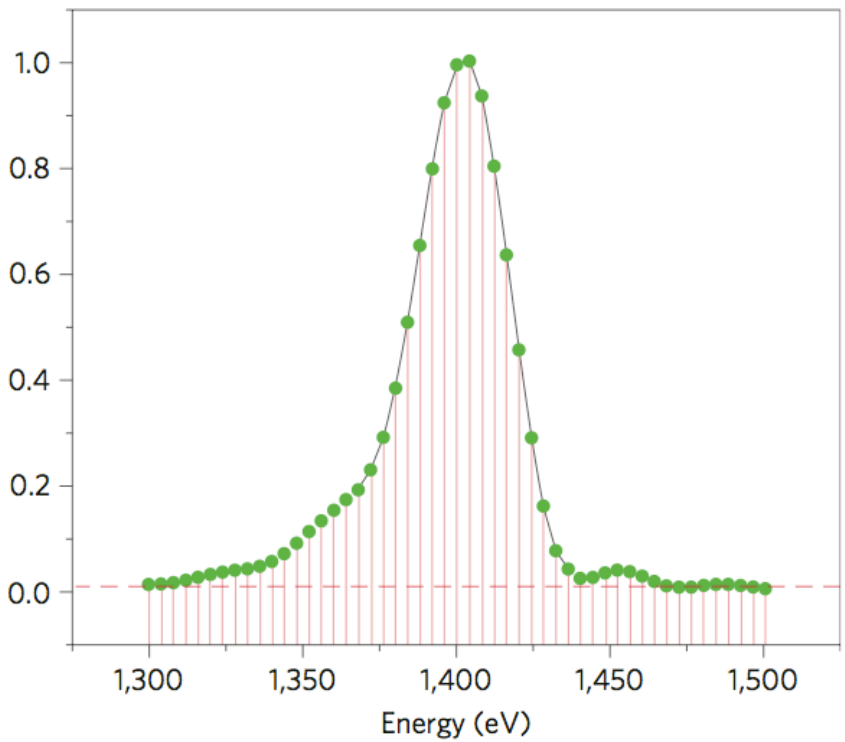

Use of entire first undulator harmonic (~2.5% BW) gives 60x gain in measurement speed.

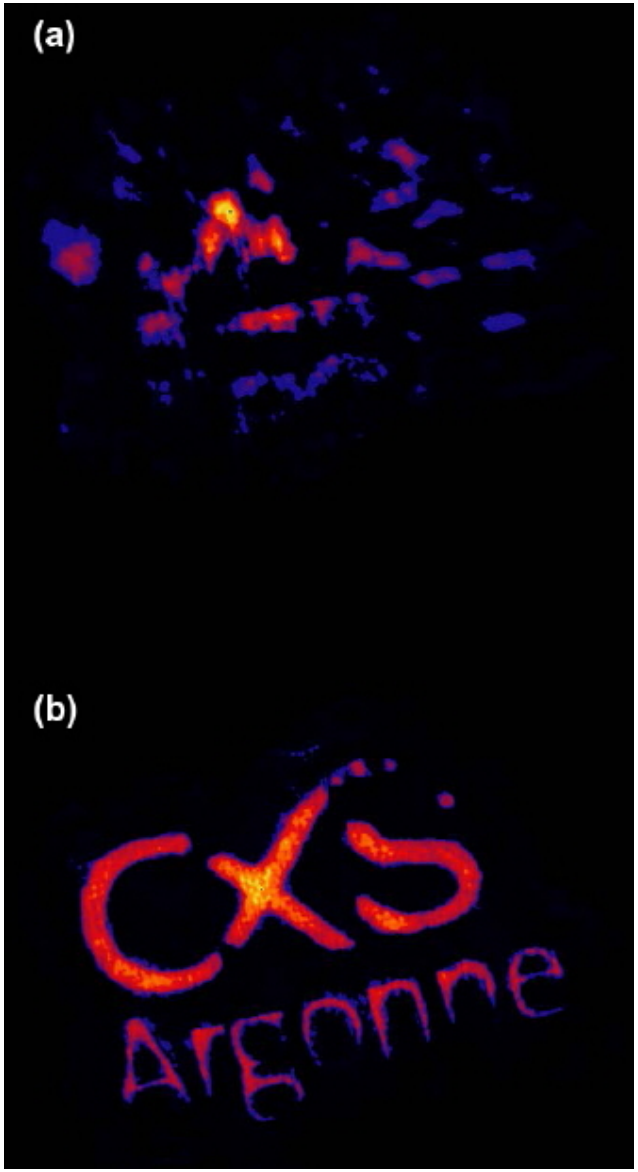

B. Abbey, Nature Photonics 5, 420 (2011)

Quantitative exploration

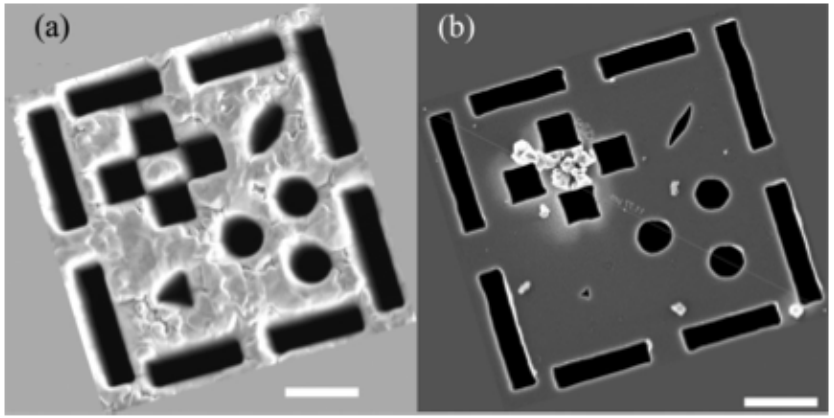

Gold test pattern

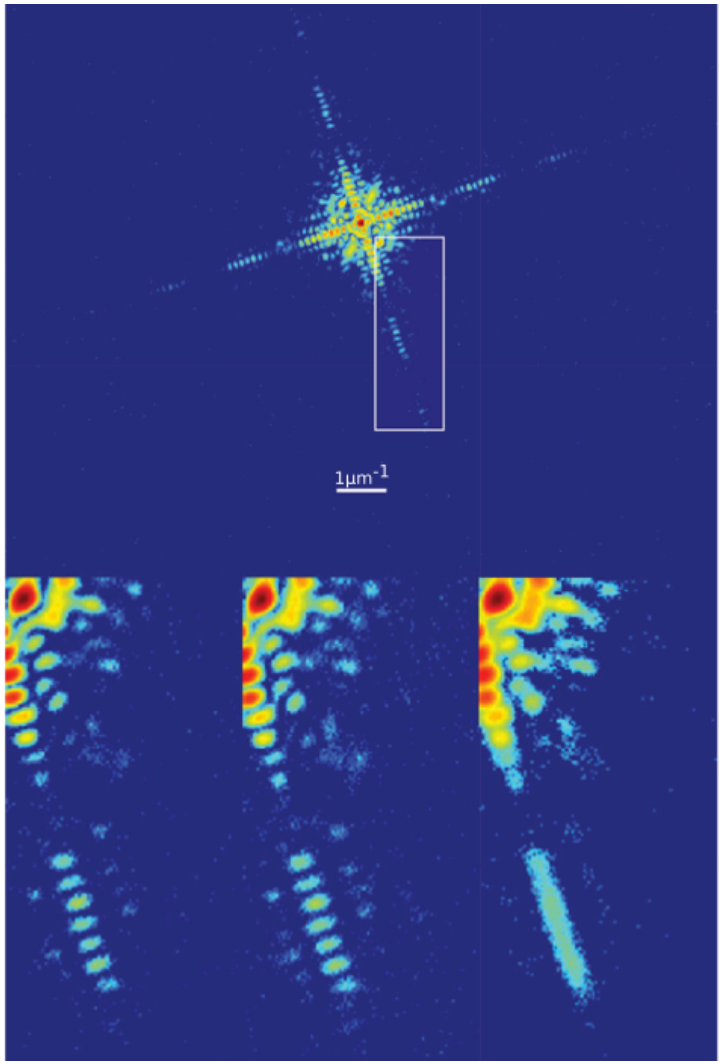

Diffraction pattern (1.4 keV) recorded with decreasing degree of coherence (open up the beamline slits)

Limits of partial coherence on phase recovery

$$S_s = \frac{\sigma_{s,x}}{2L} \qquad S_l = 2\sigma_l \frac{\delta}{\lambda L}$$

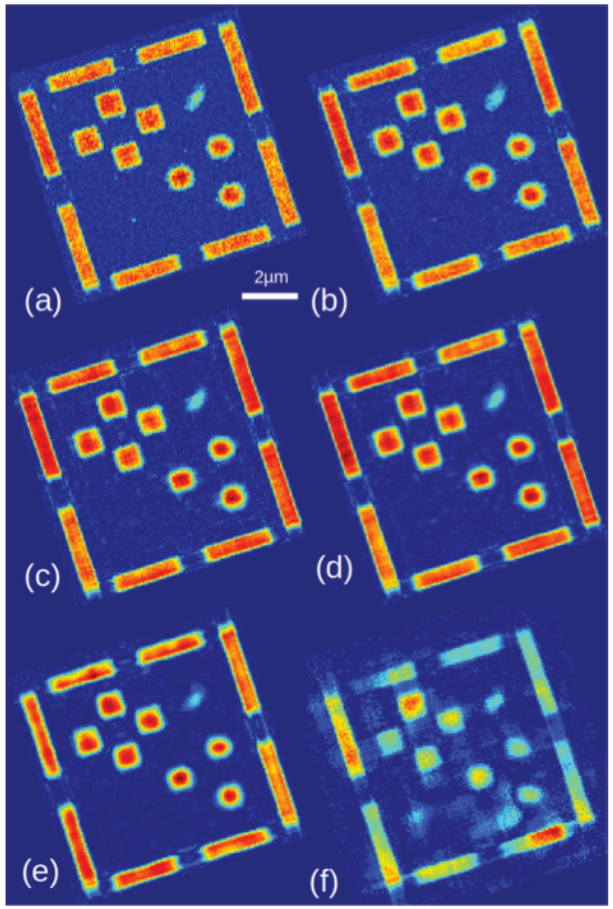

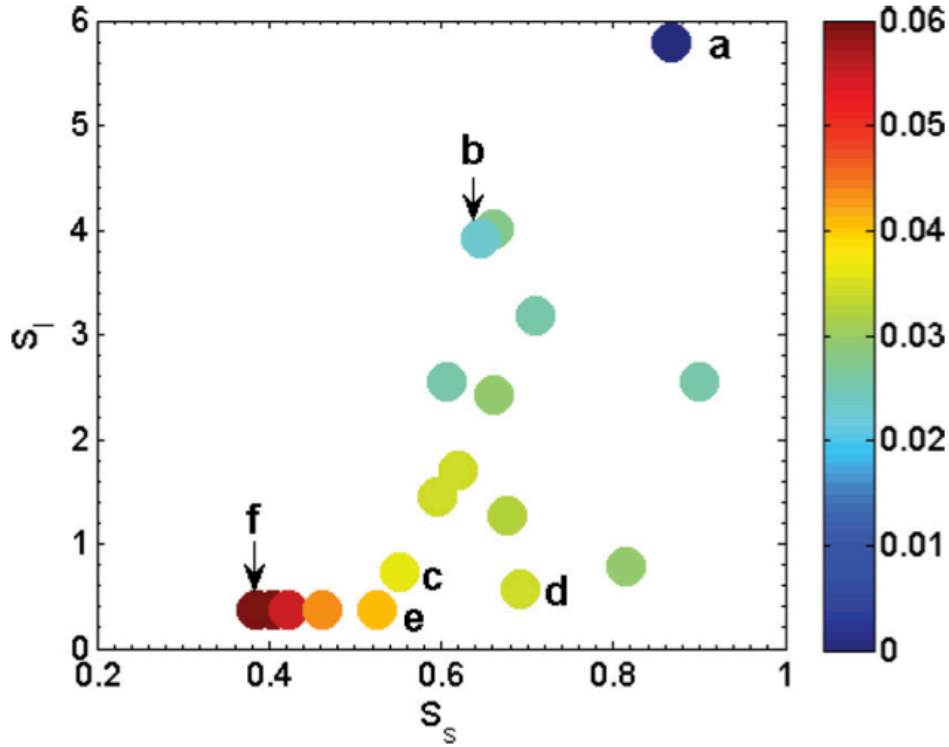

B. Chen, PRB 86, 235401 (2012)

Approach is more general than it might appear

- Fringe blurring can also be thought of as being due to sample vibration, drift, detector resolution function, etc.
- New methods for handling blurring (e.g. Gaussian approx., quantum state approach), look even more promising.
- These methods seem to work best when the number of modes ≤ 10
  -> well suited to hard x-rays from an MBA lattice

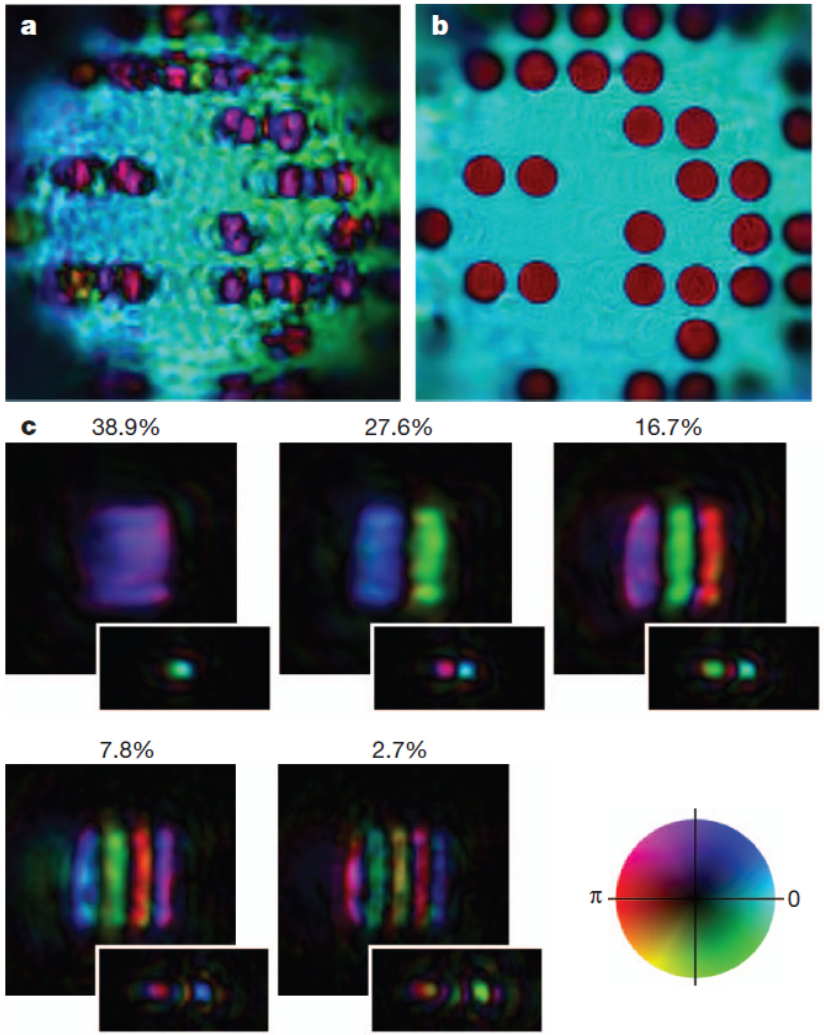

J. Clark, Nature Comms. 3, 993 (2012)
P. Thibault, Nature 494, 68 (2013)
J. Clark, PRL 112, 113901 (2014)

Coherent optics/beamlines presented at XRM 2014

http://www.xrm2014.com/

1530	Tue 8: High Brilliance	Rm: 203/4 Chair: Qun Shen
1530	**Maya Kiskinova** – X-Ray Microscopy with Synchrotron and FEL: Synergies and New Frontiers	
1610	**Christoph Quitmann** – Better Microscopy Needs Better Sources – Max IV!	

1530	Mon 4: Optics	Chair: Yoshio Suzuki Rm: 203/4
1530	**Anne Sakdinawat** – Advances in Hard X-Ray Diffractive Optics	
1610	**Istvan Mohacsi** – Double-Sided Fresnel Zone Plates	
1630	**Sven Niese** – Crossed Partial Multilayer Laue Lenses for X-Ray Imaging and Focusing Application	

1340	Mon 3A: Optics Rm: 203 Chair: Hanfei Yan
1340	**Markus Osterhoff** – Multi-Order Hard X-Ray Imaging with Multilayer Zone Plate
1400	**Sasa Bajt** – High NA Multilayer Laue lenses
1420	**Gung-Chian Yin** – Hard X-Ray Nanoprobe by Nested Montel Mirrors Aimed for 40nm Resolution at TPS
1440	**Hidekazu Takano** – Total Reflection Zone Plates for Hard X-Ray Nanofocusing

Coherence applications presented at XRM 2014

0900	Mon 1: Introduction Chair: Keith Nugent Rm: 203/4
0900	**Andrew Peele & Chris Ryan** – Welcome and Opening Remarks
0920	**Vanessa Wood** – X-Ray Microscopy Guiding the Development of Better Batteries
1000	**David Shapiro** – Soft X-Ray Ptychography for Nano-Materials Research

1100	Wed 10A: Ordered Materials Rm: 203 Chair: Brian Abbey	Wed 10B: Tomography Rm: 204 Chair: Changyong Song
1100	**Felix Hofmann** – Micro-Beam Characterisation of Lattice Distortions Due to an Individual Dislocation	**Henning Osholm Sorensen** – Multiscale Imaging of Chalk, a Natural Porous Material
1120	**Jose Avila** – Electronic Structure of Smart Low-D Materials by Nano-ARPES: Graphene, BN, MoS2,	**Huaidong Jiang** – 3D High-Resolution Quantitative Imaging of Functional Materials with Coherent X-Rays
1140	**Martin Holt** – Strain Imaging of Nano Semiconductor Heterostructures with Bragg Projection Ptychography	**Martin Dierolf** – Ptychographic X-Ray Nanotomography as a Tool for Bone Research
1200	**Tomas Stankevic** – Strain Mapping with a Nano-Focused X-Ray Beam	**Kevin Mader** – Tackling Genomics with X-Ray Micro-Tomography: A Study of Bone Microstructure

Coherence developments presented at XRM 2014

THURSDAY 30 OCTOBER		Level 2
0830	Registration & Information	
0900	Thu 11: Bio/Imaging	Rm: 203/4 Chair: Stefan Vogt
0900	**Chikara Sato** – Electron Microscopy of Proteins and Cells in Water and Ice	
0930	**David Vine** – Simultaneous Cryo X-ray Ptychography and Fluorescence	
1000	**Ismo Vartiainen** – Zernike Phase Contrast in Full-Field, Scanning, and Ptychographic X-Ray Microscopy	
1030	Morning Tea, Exhibition and Poster Viewing	
1100	Thu 12A: Bio/Imaging Rm: 203 Chair: Renzhong Tai	Thu 12B: Phase Rm: 204 Chair: Graeme Morrison
1100	**Andre Yaroshenko** – In-Vivo Lab X-Ray Dark-Field Imaging of Micro-Morphological Changes	**Tim Salditt** – Holographic Imaging Optimized by X-Rays Waveguides: Towards the Living Cell
1120	**Stephen Dubsky** – Low Dose, High Spatio-Temporal Resolution Imaging of Real-Time 4D Lung Function	**Martin Krenkel** – Holographic Zoom Tomography for Imaging of Whole Organs Down to Single Cells
1140	**Duane Loh** – Sparse, Incomplete Data from X-Ray Free-Electron Lasers	**Irene Zanette** – Recent Developments in Speckle-Based Multimodal X-Ray Imaging
1200	**Tomas Ekeberg** – Imaging of Single Biological Particles at LCLS	**Timur Gureyev** – Duality between Noise and Spatial Resolution in Linear Imaging Systems

1340	Thu 13A: Bio/Imaging Rm: 203 Chair: Hans Hertz	Thu 13B: Ptychography Rm: 204 Chair: Cameron Kewish
1340	**Changyong Song** – Multimodal Nanoscale Imaging Using Coherent X-Rays from XFEL and Synchrotron	**Marco Stockmar** – 2D and 3D Nano-Imaging Using Near-Field Ptychography
1400	**Andrew Martin** – Radiation Damage in Bioimaging with X-Ray Free-Electron Lasers	**Ana Diaz** – Quantitative Imaging of Frozen Hydrated Cells with Hard X-Ray Nanotomography
1420	**Mateusz Czyzycki** – X-Ray Fluorescence Imaging of Human Brain Cancers	**Akihiro Suzuki** – Hard X-Ray Ptychography of Extended Thick Objects Using Multislice Approach
1440	**Daniel Larsson** – Bio-Imaging with Liquid-Metal-Jet X-Ray Sources	**Harry Quiney** – Nano-Roughness and Thickness Distributions Using Broadband X-Ray CDI
1500	Afternoon Tea, Exhibition and Poster Viewing	
1530	Thu 14: Recog+Ptychog	Chair: Andrew Peele Rm: 203/4
1530	**Steve Wilkins Memorial** – Andrew Stephenson	
1540	**Alan Michette Memorial** – Graeme Morrison	
1550	**Pierre Thibault** – X-Ray Ptychography: State of the Art, Challenges, and Opportunities	